Bacteriol. **176**, 269 (1994).
18. R. J. C. McLean, M. Whiteley, D. J. Stickler, W. C. Fuqua, *FEMS Microbiol. Lett.* **154,** 259 (1997).
19. J. P. Pearson, E. C. Pesci, B. H. Iglewski, *J. Bacteriol.* **179**, 5756 (1997).
20. J. M. Brint and D. E. Ohman, *ibid.* **177**, 7155 (1995).
21. We constructed the plasmid pMRP9-1 by cloning an ~0.8-kb Kpn I–Hind III fragment containing the *Aequorea victoria* GFP gene from pGFPmut2 [B. P. Cormack, R. H. Valdivia, S. Falkow, *Gene* **173,** 33 (1996)] into Kpn I–Hind III–digested pUCP18. This places the GFP gene under control of the *lac* promoter and the T7*gene*10 ribosomal binding site. pMRP9-1 confers resistance to carbenicillin. The excitation maximum for this mutant GFP protein is 481 nm and the emission maximum is 507 nm.
22. T. A. Fassel, M. J. Schaller, C. C. Remsen, *Microbiol. Res. Tech.* **20**, 87 (1992).
23. Synthetic $3OC_{12}$-HSL (10 μM) was added to the sterilized medium just before use. The bioreactors were then inoculated with the appropriate strain of *P. aeruginosa*. Fresh medium was prepared daily to minimize any chemical degradation of the $3OC_{12}$-HSL.
24. I. W. Sutherland, in *Surface Carbohydrates of the Prokaryotic Cell*, I. W. Sutherland, Ed. (Academic Press, London, 1977), pp. 27–96.
25. P. K. I. Kintner and J. P. V. Buren, *J. Food Sci.* **47**, 756 (1982).
26. L. R. Evans and A. Linker, *J. Bacteriol.* **116,** 915 (1973).
27. M. K. Dubois, A. Gilles, J. K. Hamilton, P. A. Rebers, F. Smith, *Anal. Chem.* **28,** 350 (1956).
28. M. L. Brown, H. C. Aldrich, J. L. Gautier, *Appl. Environ. Microbiol.* **61**, 187 (1995).
29. A. E. Khoury, K. Lam, B. D. Ellis, J. W. Costerton, *Am. Soc. Artif. Intern. Organs J.* **38**, 174 (1992).
30. R. G. Dogget, G. M. Harrison, R. N. Stillwell, E. S. Wallis, *J. Pediatr.* **68,** 215 (1966).
31. All experiments were performed in EPRI medium, which contained 0.005% sodium lactate, 0.005% sodium succinate, 0.005% ammonium nitrate, 0.00019% KH_2PO_4, 0.00063% K_2HPO_4 (pH 7.0), 0.001% Hutner salts [G. Cohen-Bazire, W. R. Sistrom, R. Y. Stanier, *J. Cell. Comp. Physiol.* **49**, 35 (1957)], 0.1% glucose, and 0.001% L-histidine. Carbenicillin (150 μg/ml) was used to maintain pMRP9-1. A continuous-culture bioreactor was configured as a once–flow-through system [D. G. Davies, A. M. Chakrabarty, G. G. Geesey, *Appl. Environ. Microbiol.* **59,** 1181 (1993)]. Medium was pumped from the reservoir through the bioreactor at a flow rate of 0.13 ml/min. The flow was laminar with a Reynolds number of 0.17 and a fluid resistance time of 0.43 min. The bioreactor was composed of polycarbonate with a glass coverslip affixed to its top. This glass coverslip served as a substratum. *Pseudomonas aeruginosa* was introduced into the stream through a septum located 1 cm upstream of the bioreactor.
32. An Olympus BH2 microscope with a 60× S PlanApo objective lens was used for epifluorescence and phase-contrast microscopy. Transmitted light images were collected with an Optronics charge-coupled device (Optronics Engineering, Goleta, CA) and the imaging program Image-Pro Plus 3.0 for Windows 95 (Media Cybernatics, Silver Spring, MD). Scanning confocal microscopy was performed with a Bio-Rad MRC600 confocal microscope (Hercules, CA). The excitation band was 488 nm with a 514-nm cutoff. The 50× ULWD Olympus objective lens was used for scanning confocal microscopy. The imaging software was Comos 7.0 (Bio-Rad). The images were constructed with the SLICER imaging program (Fortner Research, Sterling, VA). The Kalman for each cross section was 5.
33. The nearest-neighbor analyses were on transmitted-light images of bacteria attached to the substratum after 10 days of continous culture. A minimum of 3000 cells in 10 fields were analyzed for each population. The distance of the nearest cell centroid to each study cell centroid was measured, and the average nearest-neighbor distance was calculated. This analysis was developed by G. Harkin (Montana State University, Bozeman, MT).
34. Biofilms for chemical analysis were grown in silicone tubing in a once-through continuous-flow system. Size 15 silicone tubing with a flow rate of 0.13 ml/min or size 15 tubing with a flow rate of 0.8 ml/min was used. After biofilms matured, the tubing was sliced lengthwise and biofilm cells were collected. The collected material was centrifuged at 13,000 rpm (Eppendorf Microfuge) for 10 min and the sedimented material was analyzed for total carbohydrates, uronic acids, and protein as described (*25*, *27*).
35. SDS (0.2% w/v) in 10 ml of EPRI medium was filtered through a 0.2-μm polycarbonate filter. After the flow of medium into the bioreactor was stopped, the SDS was injected through the septum into the flow chamber. The SDS remained in the bioreactor for 30 min, and then the flow of fresh medium was reinitiated.
36. We thank D. Ohman for providing the *rhlI* mutant PDO100, B. Cormack and S. Falkow for providing pGFPmut2, T. Moninger for assistance in preparation of the micrographs, A. Kende for synthetic $3OC_{12}$-HSL, L. Loetterle for technical assistance, and T. de Kievit for helpful discussions. Supported by Office of Naval Research grant N00014-5-0190 and a grant from the Cystic Fibrosis Foundation (E.P.G.), NIH grant AI33713 (B.H.I.), and cooperative agreement ECD-8907039 with the Engineering Research Centers and Education Division of NSF (J.W.C.). M.R.P. is an NIH Postdoctoral Fellow (GM 18740), and J.P.P. is an NIH Predoctoral Trainee (5T32AI07362).

20 November 1997; accepted 20 February 1998

Coupling Termination of Transcription to Messenger RNA Maturation in Yeast

Charles E. Birse,* Lionel Minvielle-Sebastia, Barbara A. Lee, Walter Keller, Nick J. Proudfoot†

The direct association between messenger RNA (mRNA) 3′-end processing and the termination of transcription was established for the *CYC1* gene of *Saccharomyces cerevisiae*. The mutation of factors involved in the initial cleavage of the primary transcript at the poly(A) site (*RNA14*, *RNA15*, and *PCF11*) disrupted transcription termination at the 3′ end of the *CYC1* gene. In contrast, the mutation of factors involved in the subsequent polyadenylation step (*PAP1*, *FIP1*, and *YTH1*) had little effect. Thus, cleavage factors link transcription termination of RNA polymerase II with pre-mRNA 3′-end processing.

Polyadenylation signals at the 3′ end of pre-mRNA are required for the termination of transcription in higher eukaryotes (*1*), budding yeast (*2*), and fission yeast (*3*). This ensures that transcription will only terminate after RNA polymerase II (pol II) has read beyond the end of the mRNA sequence. The mechanism of pre-mRNA 3′-end formation (sequential endonucleolytic cleavage and polyadenylation) and many of the factors involved in catalyzing these reactions are very similar between higher eukaryotes and *S. cerevisiae* (*4*). Reconstitution of this reaction in vitro in *S. cerevisiae* has allowed the fractionation of factors [cleavage factor IA (CF IA), CF IB, CF II, polyadenylation factor I (PF I), and poly(A) polymerase (PAP)] required for each step in the 3′-end formation reaction (*5*). The use of temperature-sensitive (ts) mutants has facilitated the determination of the molecular composition of these factors and revealed interactions between them (*6*). Here, we used yeast strains carrying these ts mutant alleles to demonstrate that some of these factors are also involved in pol II transcription termination.

We used transcription run-on analysis to measure transcription termination at the 3′ end of the *S. cerevisiae CYC1* gene (Fig. 1), for which signals that direct 3′-end formation have been well characterized (*7*). To achieve high transcription, we transformed yeast cells (*8*) with the multicopy plasmid pGCYC, in which the *CYC1* promoter has been replaced by the *GAL1/10* promoter region (*9*). Reverse transcription polymerase chain reaction (RT-PCR) analysis confirmed that transcripts initiating at the *GAL* promoter are polyadenylated at the same sites as found for the intact *CYC1* gene (*10*, *11*). The distribution of run-on transcript over the contiguous single-stranded probes 1 to 6 showed that transcription stops efficiently, soon after the *CYC1* poly(A) site (located at the 3′ end of probe 2), with only small amounts of run-on transcript detected beyond probe 3 (Fig. 1, B and D). This finding is in agreement with previous in vivo data showing that signals 100 base pairs (bp) beyond the *CYC1* poly(A) site are required to direct the termination of transcription (*2*). The background signal detected in the upstream *GAL* probe indicates that transcription begins at the *GAL* promoter. A similar distribution of polymerases was observed with the genomic copy of the *CYC1* gene, al-

C. E. Birse, B. A. Lee, N. J. Proudfoot, Sir William Dunn School of Pathology, South Parks Road, University of Oxford, Oxford OX1 3RE, UK.
L. Minvielle-Sebastia and W. Keller, Department of Cell Biology, Biozentrum, University of Basel, Klingelbergstrasse 70, CH-4056 Basel, Switzerland.
*Present address: Department of Biological Chemistry, 240 D Med Sci I, College of Medicine, University of California, Irvine, CA 92697, USA.
†To whom correspondence should be addressed. E-mail: nicholas.proudfoot@path.ox.ac.uk

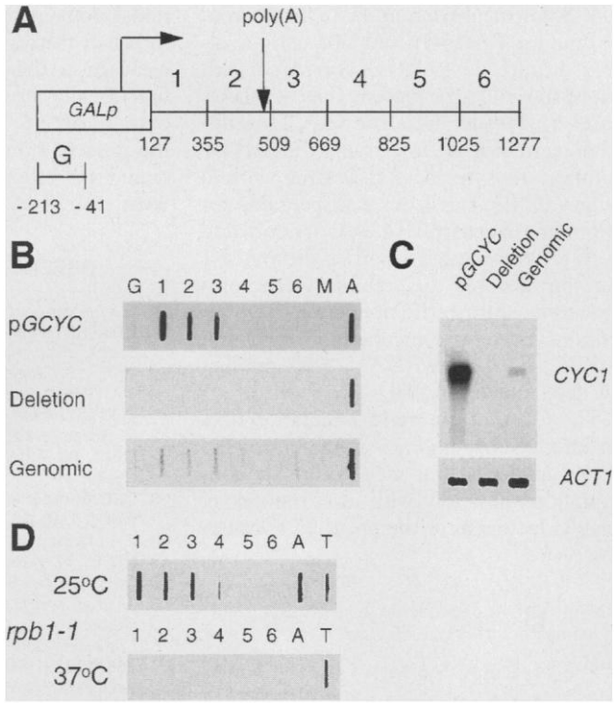

Fig. 1. Pol II transcription terminates close to the *CYC1* poly(A) site. (**A**) Schematic representation of plasmid pGCYC (*9*) showing the arrangement of M13 probes (*20*) used in run-on analysis relative to the *CYC1* poly(A) site (position 502). Locations of *CYC1* probes 1 to 6 and the upstream *GAL* probe (G) are shown relative to the *CYC1* ORF start site (position 1). (**B**) Run-on analysis across the 3′ end of the *CYC1* gene in strains indicated. Hybridization of transcripts to actin (A) and M13 control (M) probes are shown. (**C**) Northern blot analysis showing amount of *CYC1* mRNA in strains shown. The *CYC1* probe was generated by random-primer labeling of a 382-bp fragment spanning M13 probes 1 and 2. The filter was stripped and reprobed for *ACT1* mRNA as a loading control. The *ACT1* probe was generated by random-primer labeling of a 567-bp fragment spanning the M13 actin probe. (**D**) Run-on analysis across the 3′ end of the *CYC1* gene performed in the pol II temperature-sensitive strain (*rpb1-1*) under permissive (25°C) or restrictive (37°C) conditions. Hybridization of pol III transcripts to the tRNA probe (T) is shown. Transcription run-on and Northern blot analysis were performed as described (*3*). The conditions used in the run-on assay (0.5% Sarkosyl) inhibit transcription initiation but allow elongation over a short distance. Incorporation of [α-^{32}P]uridine triphosphate into nascent transcripts reflects the relative density of active RNA-polymerase complexes. After partial hydrolysis, hybridization of these end-labeled primary transcripts to single-stranded probes reveals where polymerase density falls to zero, indicating that transcription has stopped.

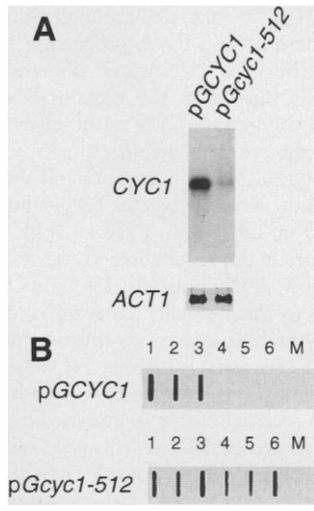

Fig. 2. Pre-mRNA 3′-end formation signal directs transcription termination. (**A**) Northern blot analysis showing *CYC1* mRNA in strains carrying either pGCYC1 or pGcyc1-512. The filter was stripped and reprobed for *ACT1* mRNA as a loading control. (**B**) Run-on analysis across 3′ end of the *CYC1* gene in strains indicated.

though the signal was 5% of that detected with the pGCYC plasmid. No signals were detected using the *CYC1* deletion strain (B-7467) (*12*). In all strains tested, polymerase density showed a strong correlation with the amount of stable *CYC1* pre-mRNA (Fig. 1C). Run-on analysis was also performed in the *rpb1-1* mutant strain that carries a ts mutation in the large subunit of RNA pol II (*13*). Inactivation of pol II activity, achieved by culturing cells at the restrictive temperature (37°C) for 60 min, abolished signals over *CYC1* (1 to 6) and *ACT1* probes that detect pol II transcription, whereas the amount of pol III–generated transcript, detected over the tRNA probe, remained unchanged (Fig. 1D).

Next, we mutated the *CYC1* polyadenylation signal to test for an effect on transcription termination. The 38-bp deletion mutation of pGcyc1-512, which prevents *CYC1* polyadenylation (*14*), also affected the termination of pol II transcription, confirming previous in vivo data (*2*). Steady-state RNA analysis (Fig. 2A) showed that the amount of stable *CYC1* transcript decreased in the strain carrying pGcyc1-512, but this analysis did not reveal the location or efficiency of transcription termination. In contrast, run-on analysis showed a marked shift in the distribution of polymerase density when the polyadenylation signal was mutated, with an increase in active polymerase complexes located well beyond the normal site of transcription termination (Fig. 2B).

Because the efficiency of mammalian pre-mRNA 3′-end formation has been correlated with the degree of transcription termination, 3′-end formation factors have been implicated in the coupling of pol II termination with RNA processing (*15*). We therefore analyzed yeast strains carrying ts mutations in the 3′-end RNA processing factors (Fig. 3). Consistent with the results of previous studies (*6*, *16*), switching growth from permissive (25°C) to restrictive conditions (37°C) severely affected the extent of pre-mRNA 3′-end formation observed in all of the mutant strains, with the amount of stable *CYC1* transcript decreasing substantially within 25 min (Fig. 3A). However, only a subset of these mutations—*rna14*, *rna15*, and *pcf11* (protein 1 of CF I)—also affected transcription termination (Fig. 3B), with considerable run-on transcript detected over probes 4, 5, and 6. With the *pap1* [poly(A) polymerase], *fip1* [factor interacting with poly(A) polymerase], and *yth1* (yeast 30-kD homolog) mutant strains, we observed little difference in polymerase density after culture in the permissive and restrictive conditions. Slightly slower decay profiles were observed with the *fip1-1* and *yth1-1* alleles (Fig. 3A); however, even after extended incubation at 37°C, no difference was observed in the polymerase profiles (*11*). The major poly(A) binding protein, Pab1p, is associated with CF IA and functions in controlling the length of the poly(A) (*17*). However, extended incubations of the ts mutant allele *pab1*-F364L (*18*) in nonpermissive conditions does not influence the polymerase profile at the 3′ end of the *CYC1* gene (*11*).

RNA14, *RNA15*, and *PCF11* are components of CF IA (Fig. 3C), a factor required for both the cleavage of the pre-mRNA and subsequent polyadenylation (*6*). In contrast, *YTH1* and *FIP1*, components of PF I and *PAP1*, are involved in the addition of the poly(A) (Fig. 3C) (*6*). This analysis therefore demonstrates that only factors involved in the pre-mRNA cleavage reaction play a role in directing termination of pol II transcription. Factors involved in polyadenylation do not appear to be required for termination.

The mammalian cleavage and polyadenylation specificity factor (CPSF) and cleavage stimulation factor (CstF) are associated with the COOH-terminal domain of the largest pol II subunit (*19*). This raised the possibility that the termination of tran-

scription might be signaled through the release of these 3′-end RNA processing factors from the COOH-terminal domain to the poly(A) signals on the nascent RNA. Therefore, the ts mutations in the cleavage factors might prevent termination through loss of poly(A) site binding. The *RNA15* gene product, Rna15p, is the only subunit of CF 1A that cross-links to RNA, binding to uridine-rich sequences like those found in yeast poly(A) signals (6). It is also homologous to mammalian cleavage factor CstF 64, which is known to interact with the pre-mRNA poly(A) signal (4). Therefore, the binding properties of this protein were compared with the ts mutant Rna15 protein. In vitro translated wild-type and ts mutant proteins both bound tightly to poly(U)-agarose (Fig. 4A, lanes 1 and 2), but not to poly(A), poly(C), or poly(G) (*11*). After incubation at 45°C for 10 min, the mutant Rna15-1p did not exhibit altered affinity for poly(U) compared with that of the wild-type protein (Fig. 4A, lanes 4 and 5). Furthermore, the COOH-terminal domain of Rna15p carrying the *ma15-1* mutation that replaces a leucine with a proline (CTA to CCA) is dispensable for its binding capacity (Fig. 4A, lanes 3 and 6). We finally tested whether the *ma15-1* mutation affected the stability of the protein after a shift to the nonpermissive temperature. Even after incubation for 60 min at 37°C, no loss in *RNA15* gene product was detectable (Fig. 4B).

The fact that the *ma15-1* mutation does not affect RNA binding or stability of the protein argues against models directly connecting termination with the transfer of poly(A) factors from the pol II COOH-terminal domain to nascent RNA. Instead, a subset of factors involved in catalyzing the cleavage of the primary transcript must be functionally active to direct the termination of transcription. Endonucleolytic cleavage of the nascent transcript may therefore be required for efficient pol II termination in yeast.

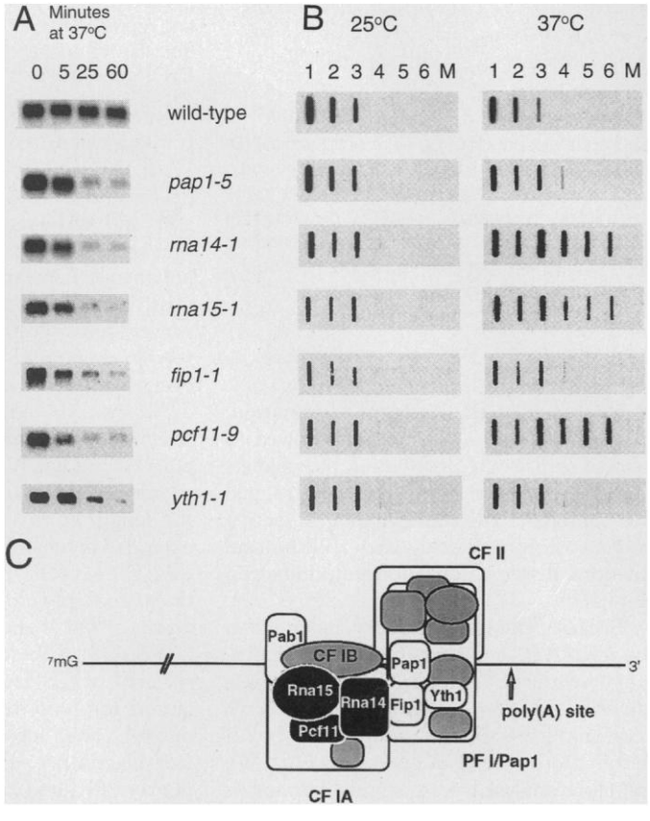

Fig. 3. Pre-mRNA 3′-end cleavage factors direct transcription termination. (**A**) Northern blot analysis showing amount of *CYC1* mRNA under permissive conditions (25°C), defined as 0, or after a shift to restrictive conditions (37°C) for 5, 25, or 60 min in strains indicated. (**B**) Run-on analysis performed under permissive conditions and after a shift to restrictive conditions for 25 min in strains indicated (*8*). (**C**) Schematic representation of proteins involved in pre-mRNA 3′-end processing in yeast. Only the proteins corresponding to the mutants tested in this study are designated.

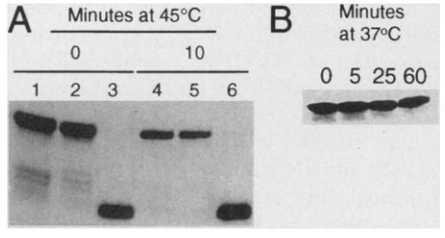

Fig. 4. Poly(U) binding of the wild-type and mutant Rna15 proteins. (**A**) The Rna15-1p produced by in vitro transcription-translation of the ts allele *rna15-1* was assayed for its ability to bind poly(U) (*21*) before or after incubation at 45°C for 10 min. Lanes 1 and 4, wild-type Rna15p; lanes 2 and 5, mutant Rna15-1 protein; lanes 3 and 6, COOH-terminal truncated version of the Rna15 protein corresponding to the RNA binding domain only (154 amino acids). (**B**) Protein immunoblot analysis showing the Rna15 mutant protein extracted from LM91 cells shifted to the nonpermissive temperature (37°C) for the times indicated. The blot was probed with antibody to Rna15p at a 1:10,000 dilution.

REFERENCES AND NOTES

1. E. Whitelaw and N. J. Proudfoot, *EMBO J.* **5**, 2915 (1986); J. Logan, E. Falck-Pedersen, J. E. Darnell, T. Shenk, *Proc. Natl. Acad. Sci. U.S.A.* **84**, 8306 (1987); S. Connelly and J. L. Manley, *Genes Dev.* **2**, 440 (1988); J. Lanoix and N. H. Acheson, *EMBO J.* **7**, 2515 (1988).
2. P. Russo and F. Sherman, *Proc. Natl. Acad. Sci. U.S.A.* **86**, 8348 (1989); P. Russo, *Yeast* **11**, 447 (1995).
3. C. E. Birse, B. A. Lee, K. Hansen, N. J. Proudfoot, *EMBO J.* **16**, 3633 (1997).
4. J. L. Manley and Y. Takagaki, *Science* **274**, 1481 (1996); W. Keller and L. Minvielle-Sebastia, *Curr. Opin. Cell Biol.* **9**, 329 (1997).
5. J. Chen and C. Moore, *Mol. Cell. Biol.* **12**, 3470 (1992).
6. L. Minvielle-Sebastia, P. J. Preker, W. Keller, *Science* **266**, 1702 (1994); P. J. Preker, J. Lingner, L. Minvielle-Sebastia, W. Keller, *Cell* **81**, 379 (1995); M. M. Kessler, J. Zhao, C. L. Moore, *J. Biol. Chem.* **271**, 27167 (1996); N. Amrani *et al.*, *Mol. Cell. Biol.* **17**, 1102 (1997); P. J. Preker, M. Ohnacker, L.Minvielle-Sebastia, W. Keller, *EMBO J.* **16**, 4727 (1997); J. Zhao, M. M. Kessler, C. L. Moore, *J. Biol. Chem.* **272**, 10831 (1997); M. M. Kessler *et al.*, *Genes Dev.* **11**, 2545 (1997); D. Patel and J. S. Butler, *Mol. Cell. Biol.* **12**, 3297 (1992); M. L. Barabino, W. Hubner, A. Jenny, L. Minvielle-Sebastia, W. Keller, *Genes Dev.* **11**, 1703 (1997).
7. Z. Guo and F. Sherman, *Trends Biochem. Sci.* **21**, 477 (1996).
8. Yeast strains were cultured in selective media (YNB) supplemented with appropriate amino acids [C. Guthrie and G. R. Fink, *Methods Enzymol.* **194**, 14 (1991)] with galactose (2%) as a carbon source. Transformation was performed as described [D. Gietz, A. St. Jean, R. A. Woods, R. H. Schiestl, *Nucleic Acids Res.* **20**, 1425 (1992)]. Strains RY260 and SB7 were transformed with plasmid pUGCYC, which carries the *URA3* (and *TRP1*) selectable marker. All other strains were transformed with pGCYC carrying *TRP1*. Conditional strains were grown at the permissive temperature (22° to 25°C) to an optical density at 600 nm of 0.1 to 0.2, briefly harvested by centrifugation (1 min), and resuspended in prewarmed media (37°C) before being cultured at the nonpermissive temperature for 5, 25, or 60 min. Formamide (2%) was added to media to restrict the function of the *fip1-1* and *yth1-1* alleles (*6*).
9. To form pGCYC, we used PCR to synthesize the region extending from 33 to 1962 bp 3′ of the *CYC1* open reading frame (ORF) start site, with genomic DNA as a template. This fragment was cloned into the unique Bgl II site of pRS424.KV, which contains the *GAL1/10* promoter region (C. Goding, unpublished data) cloned into the shuttle vector pRS424 [T. W. Christianson, R. S. Sikorski, M. Dante, J. H. Shero, P. Hieter, *Gene* **110**, 119 (1992)]. A 1480-bp fragment containing the *URA3* gene (spanning the region from 500 bp upstream of the *URA3* ORF start site to 176 bp downstream of the translation stop site) was next ligated into the Bam HI site upstream of the *GAL1/10* promoter to generate pUGCYC. pGcyc1-512 was constructed by PCR and contains the originally identified poly(A) site deletion mutation, *cyc1-512* (*14*).
10. S. Heidmann, B. Obermaier, K. Vogel, H. Domdey, *Mol. Cell. Biol.* **12**, 4215 (1992).
11. C. E. Birse, B. A. Lee, N. J. Proudfoot, L. Minvielle-Sebastia, W. Keller, unpublished data.

12. K. Barry, J. I. Stiles, D. F. Pietras, I. Melnick, F. Sherman, *Mol. Cell. Biol.* **7**, 632 (1987).
13. M. Nonet, C. Scafe, J. Sexton, R. Young, *ibid.*, p. 1602.
14. K. S. Zaret and F. Sherman, *Cell* **28**, 563 (1982).
15. G. Edwalds-Gilbert, J. Prescott, E. Falck-Pedersen, *Mol. Cell. Biol.* **13**, 3472 (1993).
16. L. Minvielle-Sebastia, B. Winsor, N. Bonneaud, F. Lacroute, *ibid.* **11**, 3075 (1991).
17. N. Amrani, M. Minet, M. Le Gouar, F. Lacroute, F. Wyers, *ibid.* **17**, 3674 (1997); L. Minvielle-Sebastia, P. J. Preker, T. Wiederkehr, Y. Strahm, W. Keller, *Proc. Natl. Acad. Sci. U.S.A.* **94**, 7897 (1997).
18. A. Sachs and J. A. Deardorff, *Cell* **70**, 961 (1992).
19. S. McCracken *et al.*, *Nature* **385**, 357 (1997); J.-C. Dantonel, K. G. K. Murthy, J. L. Manley, L. Tora, *Nature* **389**, 399 (1997).
20. The six contiguous M13 clones spanning the 3′ end of the *CYC1* gene were constructed from PCR products with pGCYC as a template. The 172-bp *GAL* probe, used to detect transcripts upstream of the *GAL* promoter, was generated with pGCYC as a PCR template. The tRNA probe was generated with genomic DNA as a PCR template. This 225-bp fragment spans the *SUP11* gene coding for Tyr-tRNA located on chromosome 6. The actin *ACT1* probe was generated as a 567-bp fragment encompassing the region 277 to 844 bp 3′ of the *ACT1* ORF start site. All fragments were cloned into M13mp19 (RF) restricted with Hinc II. The M13 control probe has no insert.
21. The wild-type Rna15p and temperature-sensitive Rna15-1p proteins were synthesized in vitro in rabbit reticulocyte lysates with [^{35}S]methionine. After incubation for 10 min at 45°C, they were assayed for their ability to bind to agarose-bound poly(U) for 15 min, as described [M. S. Swanson and G. Dreyfuss, *Mol. Cell. Biol.* **8**, 2237 (1988)]. After extensive washes, the bound material was released by boiling with SDS–polyacrylamide gel electrophoresis (PAGE) loading buffer and loaded on 10% denaturing protein gels. After electrophoresis, the gels were fixed, dried, and subjected to autoradiography.
22. We thank S. Barabino, S. Butler, F. Lacroute, A. Sachs, F. Sherman, and R. Young for various yeast strains, P. J. Preker for the *pap1* mutants, and J. Mellor for plasmids. We thank D. Pritlove and members of the N.J.P. lab for critical reading of the manuscript and for their help and advice. Supported by a Wellcome Programme Grant (032773) to N.J.P. and grants by the Kantons of Basel, the Swiss National Science Foundation, and the European Union (through the Bundesamt für Bildung und Wissenschaft, Bern) to W.K.

1 October 1997; accepted 20 February 1998

Rejoining of DNA by the RAG1 and RAG2 Proteins

Meni Melek, Martin Gellert,* Dik C. van Gent

Assembly of immunoglobulin and T cell receptor genes from separate gene segments [V(D)J recombination] begins with DNA double-strand breakage by the RAG1 and RAG2 proteins, acting at a pair of recombination signal sequences (RSSs). Here, the RAG proteins are shown to reverse the cleavage reaction by joining an RSS to a broken coding sequence end. These "hybrid joints" have also been found in lymphoid cells, even when the normal pathway of DNA double-strand break repair is inactive, and can now be explained by this activity of the RAG proteins.

An essential step in the development of lymphoid cells is the recombinational joining of gene segments to form the functional immunoglobulin and T cell receptor genes (*1*, *2*). This V(D)J recombination process is initiated by the RAG1 and RAG2 proteins (*3*, *4*), which act together to cleave DNA between the RSSs and the adjoining coding segments (*5*). The resulting double-strand breaks (DSBs) have blunt-cut RSS ends (signal ends) and coding ends that are covalently sealed into DNA hairpins. Cleavage is stimulated by the small, DNA-bending high-mobility group proteins HMG1 or HMG2 (*6*) but does not require a high-energy cofactor such as adenosine triphosphate.

Subsequently, pairs of RSS ends (signal ends) and coding ends are coupled to form signal joints and coding joints (Fig. 1). These joining reactions require the presence of several ubiquitous DSB repair factors, such as XRCC4 protein and the DNA-dependent protein kinase, composed of the catalytic subunit (DNA-PK$_{CS}$) and the heterodimeric Ku protein (*7*). Signal joints usually have a precise head-to-head linkage of the RSSs, whereas coding joints frequently have lost several nucleotides or have acquired additional nontemplated (N) nucleotides inserted by terminal deoxynucleotidyl transferase (*2*). Added nucleotides complementary to the end of the coding sequence (P nucleotides) are also observed and are readily explained as resulting from asymmetric opening of the hairpin structure formed in the first step (*1*).

However, there is an alternative outcome of V(D)J recombination: A signal end can become joined to the coding end that originally flanked the other RSS, forming a "hybrid joint" (Fig. 1). Hybrid joints can account for as many as one-fifth of the total recombinants in plasmid substrates (*8*) and have been detected at lower frequencies in the antigen receptor loci (*9*). Rejoining of the original pair of signal and coding ends, to form an "open-and-shut joint," has also been observed (*8*, *10*).

Surprisingly high numbers of hybrid joints have been found in cells that are defective in DSB joining, because of mutations in the *Ku86* or *DNA-PK*$_{CS}$ genes (*11*, *12*). These results imply either that the RAG proteins themselves are able to catalyze hybrid joint formation, as has been proposed (*11*, *12*), or that a different DSB repair pathway is involved in this joining reaction.

Using a sensitive polymerase chain reaction (PCR) assay, we showed that the RAG proteins generated hybrid joints in the absence of other joining factors. After incubation of a plasmid substrate (Fig. 2A) with the RAG1, RAG2, and HMG1 proteins in the presence of Mg^{2+}, we amplified the products by PCR, using various sets of primers to identify signal joints, coding joints, and hybrid joints.

Although we did not detect any signal or coding joints (*13*), PCR products consistent with hybrid joint formation were readily detected (Fig. 2). We assayed for a product containing the 12-RSS joined to the region that originally flanked the 23-RSS and amplified the predicted product of about 241 base pairs (bp). The DNA contained a Bam HI site but not a Sal I or Sca I site (Fig. 2B), as expected for this hybrid joint. Similarly, the reciprocal product (a junction of the 23-RSS to the coding flank originally attached to the 12-RSS) was observed with the appropriate PCR primers. This 205-bp product contained sites for Sal I and Sca I but not for Bam HI (Fig. 2C), in keeping with its expected structure. We also obtained hybrid joint products using several other DNA substrates containing different sequences flanking the RSSs or with the 12-RSS in the opposite orientation (*13*), indicating that the reaction does not depend on one particular configuration around the RSSs. This joining reaction, like RAG-mediated cleavage (*5*), did not require an exogenous energy source, suggesting that the energy of a phosphodiester bond is used to generate the new bond at the RSS border. Quantitative PCR (by dilution of rearranged substrate into the reaction mixture) revealed that the RAG proteins converted about 0.5% of the input DNA to hybrid joints.

The structure of the hybrid joints linking the 23-RSS to the 12–coding flank was analyzed in more detail by cloning and sequencing (see legend to Fig. 2). Most joints resulted from exact joining of the 23-RSS to the region originally flanking the 12-RSS, without addition or loss of nucleotides. How-

M. Melek and M. Gellert, Laboratory of Molecular Biology, National Institute of Diabetes and Digestive and Kidney Diseases, National Institutes of Health, Bethesda, MD 20892–0540, USA.
D. C. van Gent, Department of Cell Biology and Genetics, Erasmus University Rotterdam, Post Office Box 1738, 3000 DR Rotterdam, Netherlands.

*To whom correspondence should be addressed. E-mail: gellert@helix.nih.gov